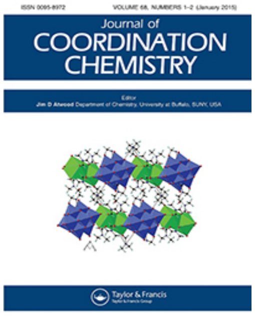

Journal of Coordination Chemistry

ISSN: 0095-8972 (Print) 1029-0389 (Online) Journal homepage: http://www.tandfonline.com/loi/gcoo20

3-D Hydrogen bonded networks of three organically templated cadmium sulfates. Dehydration reactions and crystallization behavior

Walid Rekik, Houcine Naïli & Thierry Bataille

To cite this article: Walid Rekik, Houcine Naïli & Thierry Bataille (2015) 3-D Hydrogen bonded networks of three organically templated cadmium sulfates. Dehydration reactions and crystallization behavior, Journal of Coordination Chemistry, 68:1, 142-154, DOI: 10.1080/00958972.2014.989223

To link to this article: http://dx.doi.org/10.1080/00958972.2014.989223

Journal of Coordination Chemistry, 2015
Vol. 68, No. 1, 142–154, http://dx.doi.org/10.1080/00958972.2014.989223

3-D Hydrogen bonded networks of three organically templated cadmium sulfates. Dehydration reactions and crystallization behavior

WALID REKIK†, HOUCINE NAÏLI*† and THIERRY BATAILLE‡

†Laboratoire de physico-chimie de l'État Solide, Faculté des Sciences de Sfax, Département de Chimie, Université de Sfax, Sfax, Tunisia
‡Sciences Chimiques de Rennes (CNRS, UMR 6226), Université de Rennes 1, Rennes Cedex, France

(*Received 12 April 2014; accepted 30 September 2014*)

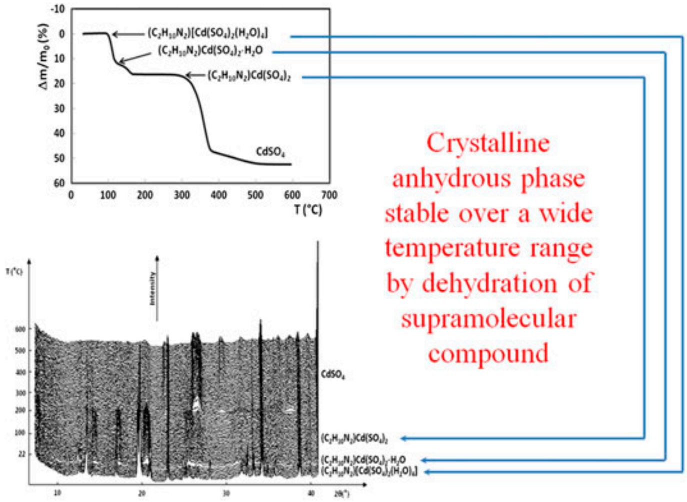

Three cadmium sulfates templated by either ethylenediamine, piperazine, or dabco, $[NH_3(CH_2)_2NH_3][Cd(SO_4)_2(H_2O)_4]$ (**1**), $(C_4H_{12}N_2)[Cd(H_2O)_6](SO_4)_2$ (**2**), and $(C_6H_{14}N_2)[Cd(H_2O)_6](SO_4)_2$ (**3**), have been synthesized and crystallographically characterized. The structural studies show that they crystallize in $P\text{-}1$, $P2_1/n$, and $P2_1/c$ space groups, respectively, and the solids present three different structure types. Thermal decomposition of all compounds depends not only on the structure type but also on the amino group involved in the structure. Three different thermal behaviors have been distinguished in the dehydration stage, which takes place in two, three, and one steps, in **1**, **2,** and **3**, respectively. The temperature-dependent X-ray diffraction demonstrates that the anhydrous compound obtained by dehydration of **1** is a crystalline phase that is stable in a wide range of temperatures.

Keywords: Hybrid material; Crystal structure; Dehydration reactions; Crystallization behavior; Cadmium

---

*Corresponding author. Email: houcine_naili@yahoo.com

1. Introduction

The chemistry of organically templated metal sulfates has received increasing attention over the last few years because of ferroelastic, ferroelectric, magnetic, and ONL properties [1–10]. A wide range of structures have been obtained, 1-D [12, 13], 2-D [11, 14–17], and 3-D [11, 17–19], all consisting of inorganic frameworks built from strong metal–oxygen bonds. Supramolecular networks of hexaaquametal sulfates including amine groups have been much less investigated although the crystal engineering of supramolecular compounds is known to favor electric and magnetic properties and compounds with hydrogen-bonded structures can lead to interesting ONL properties. In order to expand the chemistry of double sulfates of transition metal with diamine and to obtain crystals exhibiting interesting properties, we reported, recently, some new organic–inorganic hybrid solids composed of 3d transition metal, sulfate groups, and protonated diamine [20–25]. In the course of our investigations on new hybrid sulfate materials, three cadmium sulfates templated by ethylenediamine (**1**), piperazine (**2**), and dabco (**3**) have been prepared. The solids belong to three different structure types, which are described here. In addition, thermal behavior is discussed with respect to the amino group involved in the structure.

2. Experimental

2.1. *Chemical preparation*

Single crystals of the three compounds were grown as follows: 1 mM of cadmium sulfate octahydrate $3CdSO_4{\cdot}8H_2O$, 3 mM of the amine, ethylenediamine ($C_2H_8N_2$), piperazine hexahydrate ($(C_4H_{10}N_2){\cdot}6H_2O$), and 1.4-diazabicyclo[2.2.2]octane (abbreviated dabco) ($C_6H_{12}N_2$), and 3 mM of sulfuric acid H_2SO_4, for **1**, **2** and **3**, respectively, were mixed in a small amount of distilled water. The clear solutions were stirred for 15 min and allowed to stand at room temperature. After a few days, colorless single crystals were formed. The products were filtered off and washed with a small amount of distilled water. The chemical purity of the product was tested by EDAX measurements and powder X-ray diffraction for the three compounds. The three hybrid materials present similar EDAX spectra revealing the presence of all non-hydrogen atoms, Cd, S, O, N, and C. The experimental XRD powder patterns for these compounds match well with those simulated from single-crystal structure data, indicating that the compounds were isolated as single phases.

2.2. *Single-crystal diffraction data collection and structure determination*

A small crystal of each compound was glued to a glass fiber mounted on a four-circle Nonius Kappa CCD area-detector diffractometer (Center de Diffractométrie X, UMR CNRS 6226). Intensity data were collected using MoKα radiation through the program COLLECT [26]. Correction for Lorentz-polarization effect, peak integration, and background determination were carried out with DENZO [27]. Frame scaling and unit cell parameter refinement were performed with SCALEPACK [27]. Analytical absorption corrections were performed by modeling the crystal faces [28]. The main crystallographic data are listed in table 1.

Structure analyses were carried out with triclinic symmetry, space group *P-1* for **1** and with the monoclinic symmetry, space group $P2_1/n$ and $P2_1/c$ for **2** and **3**, respectively, according to the automated search for space group available in Wingx [29]. Cadmium and

Table 1. Crystallographic data for **1–3**.

Empirical formula	$C_2H_{18}CdN_2O_{12}S_2$ (**1**)	$C_4H_{24}MgN_2O_{14}S_2$ (**2**)	$C_6H_{26}MgN_2O_{14}S_2$ (**3**)
Formula	$(C_2H_{10}N_2)[Cd(SO_4)_2(H_2O)_4]$	$(C_4H_{12}N_2)[Cd(H_2O)_6](SO_4)_2$	$(C_6H_{14}N_2)[Cd(H_2O)_6](SO_4)_2$
Formula weight	438.70	500.77	526.81
Temperature (K)	293(2)	293(2)	293(2)
Crystal system	Triclinic	Monoclinic	Monoclinic
Space group	*P*-1	*P2₁/n*	*P2₁/c*
a (Å)	6.9114(2)	13.1588(2)	12.1906(2)
b (Å)	7.3056(2)	10.7024(2)	12.4540(2)
c (Å)	7.3629(1)	13.3865(2)	12.3544(2)
α (°)	74.013(2)	90	90
β (°)	71.731(1)	113.328(1)	105.048(1)
γ (°)	78.043(1)	90	90
V (Å^3)	336.39(1)	1731.12(6)	1811.35(5)
Z	1	4	4
ρ_{cal} (g cm^{-1})	2.166	1.921	1.932
Crystal size (mm^3)	0.120 × 0.105 × 0.072	0.128 × 0.101 × 0.099	0.318 × 0.251 × 0.092
Habit–color	Prism–colorless	Prism–colorless	Prism–colorless
λ (MoKα) (Å)	0.71073	0.71073	0.71073
μ (mm^{-1})	1.994	1.571	1.507
θ Range (°)	2.93–42.20	2.65–27.51	2.65–27.50
Index ranges	$-13 \le h \le 13$ $-9 \le k \le 13$ $-9 \le l \le 13$	$-17 \le h \le 17$ $-13 \le k \le 13$ $-17 \le l \le 17$	$-15 \le h \le 15$ $-16 \le k \le 16$ $-16 \le l \le 16$
Unique data	4685	3959	4070
Observed data [$I > 2\sigma(I)$]	4353	3427	3725
F (0 0 0)	220	1016	1072
Refinement method	Full matrix least-squares on $\|F^2\|$	Full matrix least-squares on $\|F^2\|$	Full matrix least-squares on $\|F^2\|$
R_1	0.0303	0.0309	0.0356
wR_2	0.0711	0.0834	0.0871
GoF	1.055	1.054	1.046
No. parameters	105	257	283
Transmission factors	0.81744 and 0.88516	0.85084 and 0.88513	0.68470 and 0.87976
Largest diff. map hole and peak (e Å^{-3})	−1.490 and 0.902	−0.614 and 0.673	−1.122 and 2.010

sulfur were located using direct methods with SHELXS-97 [30]. The oxygens and the organic moieties were found from successive Fourier calculations using SHELXL-97 [31]. The water hydrogens were located in a difference map and refined with O–H distance restraints of 0.85(2) Å and H···H restraints of 1.39(2) Å so that the H–O–H angle fitted to the ideal value of a tetrahedral angle. Hydrogens bonded to C and N were positioned geometrically and allowed to ride on their parent atoms, with C–H = 0.97 Å and N–H = 0.90 Å. Bond distances and angles calculated from the final atomic coordinates, as well as probable hydrogen bonds, are given in tables 2 and 3.

2.3. *Thermal behavior*

A thermogravimetric (TG) measurement was performed for **1** with a SETERAM TG-DTA92 instrument under flowing air, with a heating rate of 5 °C min^{-1} from ambient temperature to 600 °C. Temperature-dependent X-ray powder diffraction (TDXD) was performed with a powder diffractometer combining the curved-position-sensitive detector (CPS120) from INEL and a high temperature attachment from Rigaku. The detector was

Table 2. Bond distances (Å) and angles (°) within the cadmium octahedra CdO_6.

$(C_2H_{10}N_2)[Cd(SO_4)_2(H_2O)_4]$ (**1**)					
Cd–OW1	2.251(1)	OW1–Cd–OW1^I	180.0	OW1^I–Cd–OW2	84.99(5)
Cd–OW1^I	2.251(1)	OW1–Cd–O4	94.25(5)	OW1^I–Cd–OW2^I	95.01(5)
Cd–O4	2.2789(9)	OW1–Cd–O4^I	85.75(5)	O4–Cd–O4^I	180.0
Cd–O4^I	2.2789(9)	OW1–Cd–OW2	95.01(5)	O4–Cd–OW2	92.03(4)
Cd–OW2	2.289(1)	OW1–Cd–OW2^I	84.99(5)	O4–Cd–OW2^I	87.97(4)
Cd–OW2^I	2.289(1)	OW1^I–Cd–O4	85.75(5)	O4^I–Cd–OW2	87.97(4)
		OW1^I–Cd–O4^I	94.25(5)	O4^I–Cd–OW2^I	92.03(4)
				OW2–Cd–OW2^I	180.0

Symmetry code: ^{I} $-x+1, -y+1, -z+2$.

$(C_4H_{12}N_2)[Cd(H_2O)_6](SO_4)_2$ (**2**)					
Cd–OW1	2.248(2)	OW1–Cd–OW2	88.79(9)	OW2–Cd–OW5	89.40(9)
Cd–OW2	2.250(2)	OW1–Cd–OW3	92.15(8)	OW2–Cd–OW6	93.60(8)
Cd–OW3	2.276(2)	OW1–Cd–OW4	83.13(9)	OW3–Cd–OW4	84.64(9)
Cd–OW4	2.294(2)	OW1–Cd–OW5	92.13(9)	OW3–Cd–OW5	92.08(8)
Cd–OW5	2.297(2)	OW1–Cd–OW6	175.83(8)	OW3–Cd–OW6	85.37(8)
Cd–OW6	2.297(2)	OW2–Cd–OW3	178.21(9)	OW4–Cd–OW5	174.11(9)
		OW2–Cd–OW4	94.0(1)	OW4–Cd–OW6	93.29(9)
				OW5–Cd–OW6	91.31(8)

$(C_6H_{14}N_2)[Cd(H_2O)_6](SO_4)_2$ (**3**)					
Cd–OW1	2.241(2)	OW1–Cd–OW2	178.12(8)	OW2–Cd–OW5	87.97(8)
Cd–OW2	2.250(2)	OW1–Cd–OW3	87.87(7)	OW2–Cd–OW6	88.26(8)
Cd–OW3	2.257(2)	OW1–Cd–OW4	94.20(8)	OW3–Cd–OW4	173.09(8)
Cd–OW4	2.263(2)	OW1–Cd–OW5	91.13(8)	OW3–Cd–OW5	98.92(9)
Cd–OW5	2.315(2)	OW1–Cd–OW6	92.83(7)	OW3–Cd–OW6	88.24(7)
Cd–OW6	2.349(2)	OW2–Cd–OW3	90.64(7)	OW4–Cd–OW5	87.65(9)
		OW2–Cd–OW4	87.41(8)	OW4–Cd–OW6	85.07(8)
				OW3–Cd–OW6	171.94(8)

used in a semi-focusing arrangement by reflection (Cu Ka1 radiation, $K = 1.5406$ Å) as described elsewhere [18].

3. Results and discussion

3.1. *Crystal structures*

The crystal structure of ethylenediammonium tetraaquadisulfatocadmate(II), $[NH_3(CH_2)_2NH_3][Cd(SO_4)_2(H_2O)_4]$ (**1**), consists of $[Cd(SO_4)_2(H_2O)_4]^{2-}$, built from octahedral $Cd(H_2O)_4O_2$ and tetrahedral SO_4 units linked by corner sharing, and of ethylenediammonium cations linked to the anions via N–H···O hydrogen bonds. The asymmetric unit contains only one half of the compound with the other half related to the first by the inversion center. The crystal structure presents alternate stacking of the inorganic and organic layers along the crystallographic *b* axis. The structure cohesion and stability are further assured by O(water)–H···O hydrogen bonds [32]. The structure of **1** has already been observed in cobalt, magnesium, manganese, and iron compounds [23, 24, 33, 34].

$(C_4H_{12}N_2)[Cd(H_2O)_6](SO_4)_2$ (**2**) and $(C_6H_{14}N_2)[Cd(H_2O)_6](SO_4)_2$, (**3**), crystallize in the monoclinic system and their structures belong to the centro-symmetric space groups $P2_1/n$ and $P2_1/c$, respectively. The two crystal structure types consist of cadmium cations octahedrally coordinated by six waters, $[Cd(H_2O)_6]^{2+}$, isolated sulfate anions, SO_4^{2-}, and

Table 3. Hydrogen-bonding geometry (Å, °).

D–H···A	*d*(D–H) (Å)	*d*(H···A) (Å)	*d*(D···A) (Å)	∠D–H···A (°)
$(C_2H_{10}N_2)[Cd(SO_4)_2(H_2O)_4]$ (**1**)				
N–H0A···O4	0.89	1.93	2.815(2)	176.7
N–H0B···O2$^{\mathrm{IIX}}$	0.89	1.99	2.838(2)	159.5
N–H0C···O3$^{\mathrm{III}}$	0.89	2.03	2.876(2)	159.5
OW1–H11···O2$^{\mathrm{VI}}$	0.83(2)	1.91(2)	2.734(2)	176(3)
OW1–H12···O3$^{\mathrm{V}}$	0.85(2)	1.89(2)	2.729(2)	174(3)
OW2–H21···O1$^{\mathrm{IV}}$	0.83(2)	2.02(2)	2.818(2)	162(2)
OW2–H22···O1$^{\mathrm{VII}}$	0.84(2)	1.89(2)	2.715(2)	165(2)
Symmetry codes: $^{\mathrm{I}}\,-x+1, -y+1, -z+2$; $^{\mathrm{II}}\,-x+2, -y+2, -z+1$; $^{\mathrm{III}}\,-x+2, -y+2, -z+2$; $^{\mathrm{IV}}\,x, y, z-1$; $^{\mathrm{V}}\,x, y-1, z$; $^{\mathrm{VI}}\,-x+1, -y+1, -z+3$; $^{\mathrm{VII}}\,-x+2, -y+1, -z+2$; $^{\mathrm{IIX}}\,-x+1, -y+2, -z+2$.				
$(C_4H_{12}N_2)[Cd(H_2O)_6](SO_4)_2$ (**2**)				
N1–H1D···O7$^{\mathrm{III}}$	0.90	1.84	2.734(3)	169.2
N1–H1C···O4	0.90	1.87	2.765(3)	170.3
N2–H2D···O4$^{\mathrm{VII}}$	0.90	1.93	2.796(3)	161.9
N2–H2C···O6	0.90	1.94	2.768(3)	152.6
OW1–H11···O1$^{\mathrm{IV}}$	0.84(2)	1.90(2)	2.726(3)	168(4)
OW1–H12···O7$^{\mathrm{V}}$	0.84(2)	1.86(2)	2.698(3)	177(4)
OW2–H22···O2$^{\mathrm{VII}}$	0.85(2)	1.84(2)	2.679(3)	175(4)
OW2–H21···O1	0.84(2)	1.94(3)	2.726(3)	154(5)
OW3–H32···O8$^{\mathrm{V}}$	0.86(2)	1.87(2)	2.721(3)	173(4)
OW3–H31···O5	0.86(2)	1.85(2)	2.695(3)	170(4)
OW4–H42···O6$^{\mathrm{VI}}$	0.86(2)	1.90(2)	2.705(3)	156(4)
OW4–H41···O2	0.85(2)	1.87(2)	2.717(3)	171(4)
OW5–H51···O3$^{\mathrm{IV}}$	0.84(2)	1.98(2)	2.805(3)	170(4)
OW5–H52···O8	0.84(2)	1.89(2)	2.729(3)	176(3)
OW6–H62···O3$^{\mathrm{VII}}$	0.85(2)	1.94(2)	2.784(3)	173(4)
OW6–H61···O5$^{\mathrm{VI}}$	0.84(2)	2.27(3)	2.991(4)	144(3)
Symmetry codes: $^{\mathrm{I}}\,-x, -y+1, -z+1$; $^{\mathrm{II}}\,-x+1, -y, -z+1$; $^{\mathrm{III}}\,x+1, y, z$; $^{\mathrm{IV}}\,-x, -y, -z$; $^{\mathrm{V}}\,-x-1/2, y-1/2, -z+1/2$; $^{\mathrm{VI}}\,-x, -y, -z+1$; $^{\mathrm{VII}}\,-x+1/2, y+1/2, -z+1/2$.				
$(C_6H_{14}N_2)[Cd(H_2O)_6](SO_4)_2$ (**3**)				
N1–HN1···O6$^{\mathrm{II}}$	0.79(3)	2.01(4)	2.754(3)	156(3)
N2–HN2···O1$^{\mathrm{I}}$	0.81(4)	1.91(4)	2.671(3)	156(4)
OW1–H11···O5$^{\mathrm{III}}$	0.84(2)	1.84(2)	2.678(3)	175(4)
OW1–H12···O7$^{\mathrm{I}}$	0.85(2)	1.81(2)	2.660(3)	172(4)
OW2–H21···O2	0.84(2)	1.92(2)	2.743(3)	171(4)
OW2–H22···O4$^{\mathrm{II}}$	0.86(2)	1.83(2)	2.679(3)	175(3)
OW3–H31···O7	0.84(2)	1.89(2)	2.722(3)	173(3)
OW3–H32···O3	0.85(2)	1.88(2)	2.724(3)	173(3)
OW4–H41···O4$^{\mathrm{IV}}$	0.85(2)	1.86(2)	2.689(3)	166(4)
OW4–H42···O8$^{\mathrm{III}}$	0.85(2)	1.87(2)	2.721(3)	172(4)
OW5–H51···O6$^{\mathrm{II}}$	0.85(2)	1.96(2)	2.801(3)	171(4)
OW5–H52···O3$^{\mathrm{II}}$	0.85(2)	1.93(2)	2.780(3)	175(3)
OW6–H61···O8$^{\mathrm{I}}$	0.84(2)	1.93(2)	2.766(3)	173(4)
OW6–H62···O2$^{\mathrm{IV}}$	0.84(2)	2.05(2)	2.896(3)	179(4)
Symmetry codes: $^{\mathrm{I}}\,-x+1, -y, -z+2$; $^{\mathrm{II}}\,x, -y+1/2, z-1/2$; $^{\mathrm{III}}\,-x+1, y-1/2, -z+3/2$; $^{\mathrm{IV}}\,-x, y-1/2, -z+3/2$.				

protonated piperazine or dabco moieties, $C_4H_{12}N_2^{2+}$ or $C_6H_{14}N_2^{2+}$, in **2** and **3**, respectively. The cohesion of the structure is ensured by hydrogen bonds between the cationic groups and sulfate oxygens only. The resulting H-bonding networks can be described by 3-D supramolecular frameworks, thus forming channels in which the protonated diamine cations play a templating role. The structures can be described as alternating anionic and cationic

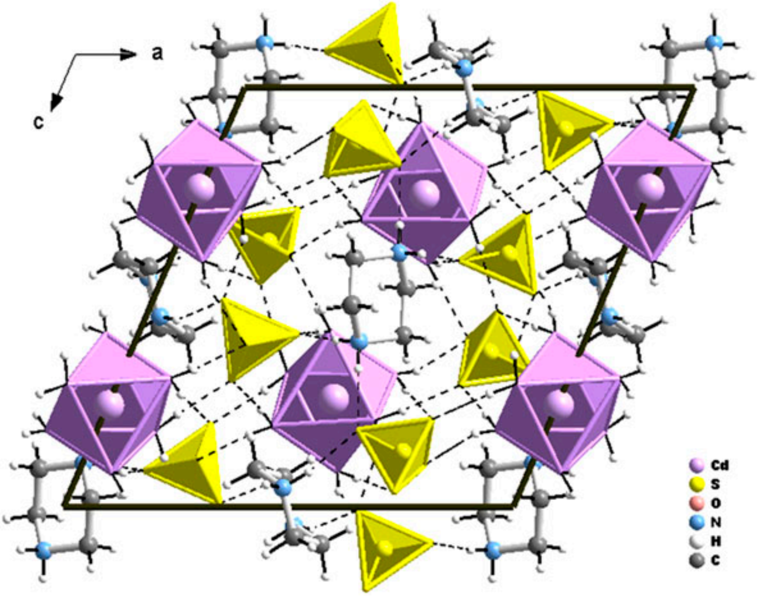

Figure 1. Projection of the structure of $(C_4H_{12}N_2)[Cd(H_2O)_6](SO_4)_2$ (**2**) along the *b* axis.

layers along the crystallographic *a*-axis for **2** and along the [0 1 0] direction for the dabco-related phase **3** (figures 1 and 2).

Contrary to **1** where the metal lies on a special position inversion center (Wyckoff site 1e), within the structures of **2** and **3**, the cadmium ions occupy general positions (Wyckoff site 4e). The substitution of the diamine, playing the role of directing agent in this family of hybrid materials, leads not only to different structure types but also to change in the coordination sphere around the metal. Indeed, in **1,** Cd has an octahedral coordination formed by two sulfates and four waters giving $[Cd(SO_4)_2(H_2O)_4]^{2-}$. In **2** and **3,** each cadmium is surrounded by six water molecules to form $[Cd(H_2O)_6]^{2+}$. The result is from the shape, size, and the connection of amino group involved in the structure. The cadmium octahedra are slightly irregular as seen in other templated metal sulfates [20–25]. Indeed, the Cd–OW distances range from 2.248(2) to 2.297(2) Å and from 2.241(2) to 2.349(2) Å in **2** and **3**, respectively (table 2). The mean values, <Cd–OW> = 2.277(2) and 2.279(2) Å, in **2** and **3**, respectively, are in agreement with the calculated ones from the bond valence program VALENCE [35] for a sixfold oxygen-coordinated Cd (2.310 Å). The Cd ions are isolated with a shortest Cd–Cd distance of 6.531(0) and 7.369(5) Å in **2** and **3**, respectively, while they are separated with the shortest intermetallic distance of 6.9114(2) Å in **1** which crystallizes in another crystal system. The shortest metal–metal distance depends not only on the size and shape of the amino group involved in these structures (dabco is bigger than piperazine which is bigger than ethylenediamine, i.e. $[H_2N(CH_2)_6NH_2]^{2+}$, $[H_2N(CH_2)_4NH_2]^{2+}$, and $[H_2N(CH_2)_2NH_2]^{2+}$) but also on the structure type. In the structure of **2,** there are two crystallographically independent piperazine molecules lying on centers of symmetry (Wyckoff sites 2a and 2b), while the dabco moiety occupies a general position in the structure of **3** although the cadmium ions are placed in general positions in both structure types. If the amine in **3** is located in a special position, it will necessarily be disordered

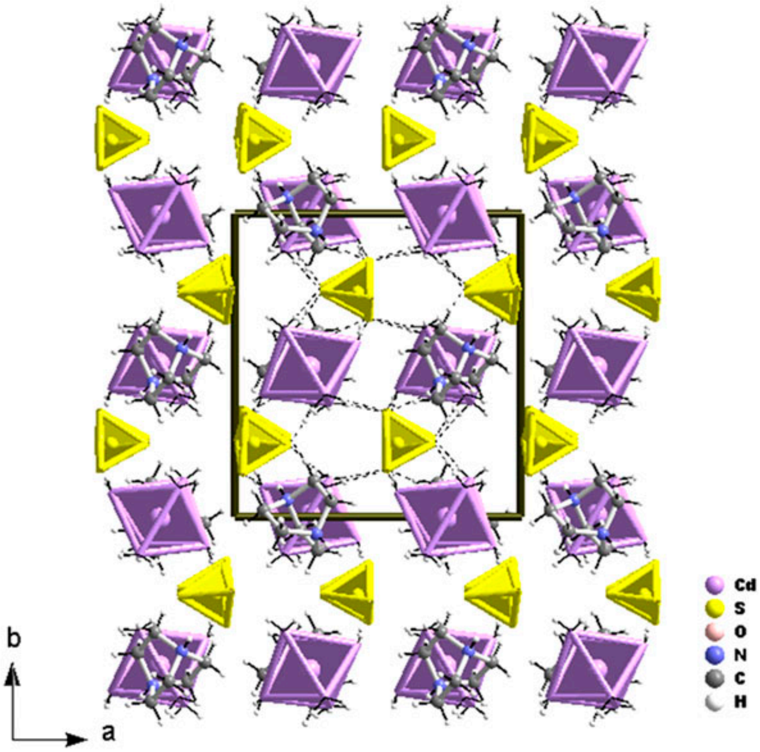

Figure 2. Projection of the structure of $(C_6H_{14}N_2)[Cd(H_2O)_6](SO_4)_2$ (**3**) along the *c* axis.

between two orientations as seen in the copper and iron-related phases [21, 36] because of its internal symmetry D_{3h}. The dihedral angle between the mean planes of the two piperazine groups observed in **2** is equal to 49.982°. The protonated diamines alternate with the metal cation along [1 1 1] and [0 2 1] in **1** and **2**, respectively, while they alternate along the three crystallographic axes in **3**. The two types of cations form mixed cationic layers parallel to the (1 0 0) and (0 1 0) plane in **2** and **3**, respectively.

Within each structure of **2** and **3**, there are two crystallographically independent sulfurs with tetrahedral coordination geometry. The sulfate tetrahedra are placed in the structure between the cationic interlayers forming anionic stacks which compensate the positive charge of the cations. Then, the structures of **2** and **3** can be described as an alternation of anionic and cationic layers along the *a* and *b* axes, respectively. The SO_4 tetrahedra play the major role in cohesion of the supramolecular networks. Indeed, the tetrahedra are H bonded to the metallic octahedra and the organic cations. Each protonated diamine (piperazine and dabco) engages hydrogens bonded to nitrogen in hydrogen bonds with sulfate. The difference between the structures **2** and **3** can be observed in the environment around cadmium. The inorganic cation $[Cd(H_2O)_6]^{2+}$ is H bonded to six sulfates in a bidentate fashion [figure 3(a)] in **2,** while it is linked via Ow–H···O hydrogen bonds to seven sulfates, five in a bidentate fashion and two monodentate in **3** [figure 3(b)]. For **1**, each cadmium octahedron shares two oxygens with two sulfates and connects six other anions by H bonds, two bidentate, and four monodentate. Within the intermolecular hydrogen bonds, the

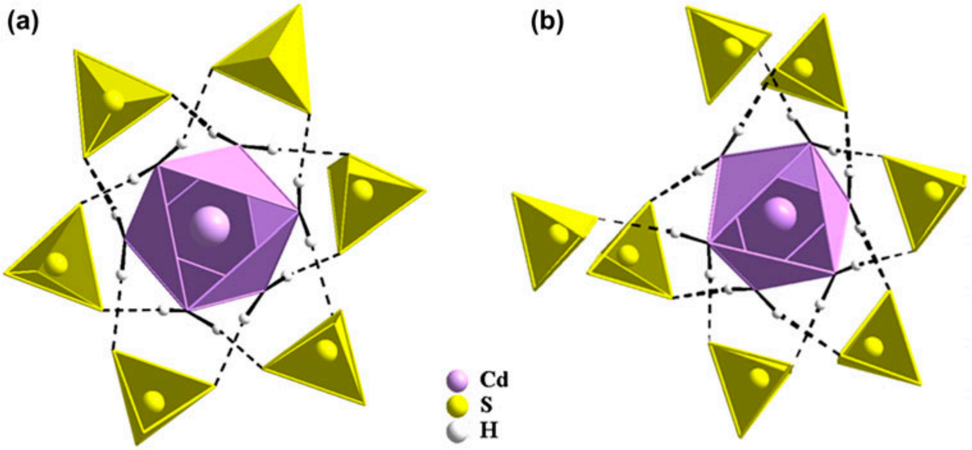

Figure 3. Neighboring sulfates in the environment of the cadmium octahedron for (a) **2** and (b) **3**.

donor–acceptor distances vary from 2.715(2) to 2.876(2) Å, from 2.679(3) to 2.991(4) Å, and from 2.660(3) to 2.896(3) Å (table 3). The mean values of the D···O distances are 2.783(2), 2.752(3), and 2.734(3) Å in **1**, **2,** and **3**, respectively, indicating that the 3-D supramolecular network of **3** is stronger than that in **2** and the weakest is in **1**. The main structural differences between the three compounds are listed in table 4.

Three structure types of cadmium sulfates templated by ethylenediamine, piperazine, or dabco are described and compared. The sizes and shapes of these three molecules are different, and the organic amines occupy different positions. Though the exact mechanism of formation is far from understood, nitrogen of the amine plays a vital role. These diprotonated organic cations not only balance the negative charge of the inorganic network, but interact with the sulfate anions through H bonding and exert a template role to direct the construction of the structures. Two parameters relative to the nature of the amine are important: the size and shape of the amine (either spherical or linear) and its ability to be protonated. Hence, the volume, the anisotropy, and the charge will influence the structure and porosity of the solid.

Table 4. The main structural differences between the three compounds.

Amine	Ethylenediamine	Piperazine	Dabco
Formula	$(C_2H_{10}N_2)[Cd(SO_4)_2(H_2O)_4]$	$(C_4H_{12}N_2)[Cd(H_2O)_6](SO_4)_2$	$(C_6H_{14}N_2)[Cd(H_2O)_6](SO_4)_2$
Crystal system	Triclinic	Monoclinic	Monoclinic
Space group	*P*-1	*P2₁/n*	*P2₁/c*
Cd position	Special	General	General
Amine position	Special	Special	General
Sulfur position	General	General	General
Cd coordination	$[Cd(SO_4)_2(H_2O)_4]^{2-}$	$[Cd(H_2O)_6]^{2+}$	$[Cd(H_2O)_6]^{2+}$
Amine-Cd alternation	[1 1 1]	[0 2 1]	*a*, *b* and *c* axes
Anionic–cationic layer alternation	[0 1 0]	[1 0 0]	[0 1 0]
Shortest Cd–Cd distance	6.9114(2) Å	6.531(0) Å	7.369(5) Å

3.2. *Thermal decompositions*

The thermal decomposition of the three compounds between room temperature and 600 °C leads to the cadmium sulfate $CdSO_4$.

3.2.1. $[NH_3(CH_2)_2NH_3][Cd(SO_4)_2(H_2O)_4]$ (1).

The TG curve of **1**, carried out with a heating rate of 5 °C min^{-1} between 30 and 600 °C, is shown in figure 4 with three successive weight losses. Figure 5 shows the 3-D representation of the powder diffraction patterns obtained during decomposition under flowing air of **1** with a heating rate of 14.4 °C h^{-1}. This plot reveals that decomposition of the precursor proceeds through several stages and confirms the thermogravimetric analysis. These experimental results can be explained as follows:

The first weight loss (of 12.14%), 95, and 135 °C, corresponds to loss of three waters (calculated weight loss, 12.30%). The TDXD plot shows that this transformation is accompanied by a change in the initial diffraction pattern. Interrogation of the ICDD powder diffraction file [37] revealed that this phase is a new one for $[NH_3(CH_2)_2NH_3]Cd(SO_4)_2{\cdot}H_2O$. This intermediate monohydrate phase is not stable and decomposes immediately by loss of the remaining water giving an anhydrous phase (observed weight loss, 16.33%; calculated weight loss, 16.41%). The second stage of dehydration is accompanied by a change in the diffraction lines, indicating a structural rearrangement. The crystalline anhydrous phase $[NH_3(CH_2)_2NH_3]Cd(SO_4)_2$ is stable in a wide temperature range; the plateau of this phase is clearly observed on the TG curve between 165 and 290 °C. Removal of the water molecules, all bonded to Cd, leads to crystalline compounds that reveal the long-range ordering of the cations and anions involved in the structure. Then a strong rearrangement occurs that allows binding of four sulfate oxygens onto Cd^{2+}. Such expectation offers potential to produce open-framework metal sulfates from supramolecular precursor. High-quality powder diffraction data for this phase were collected *in situ* at 240 °C using the Bruker D5005 diffractometer. Unfortunately, high background contribution and instability of diffracted intensities did not allow further structural investigations of the anhydrous compound. The next step of the decomposition starts at about 290 °C and corresponds to the departure of the

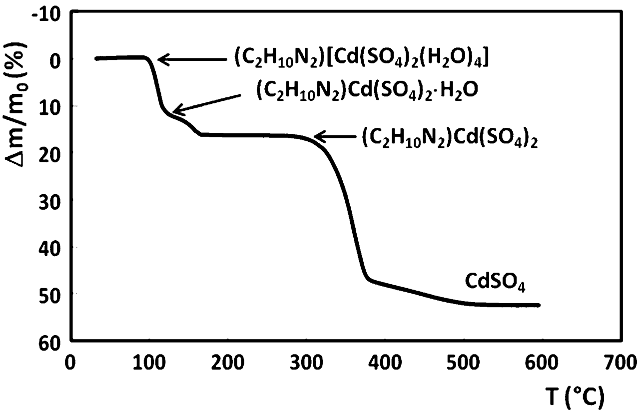

Figure 4. TG curve for the decomposition of **1** in air.

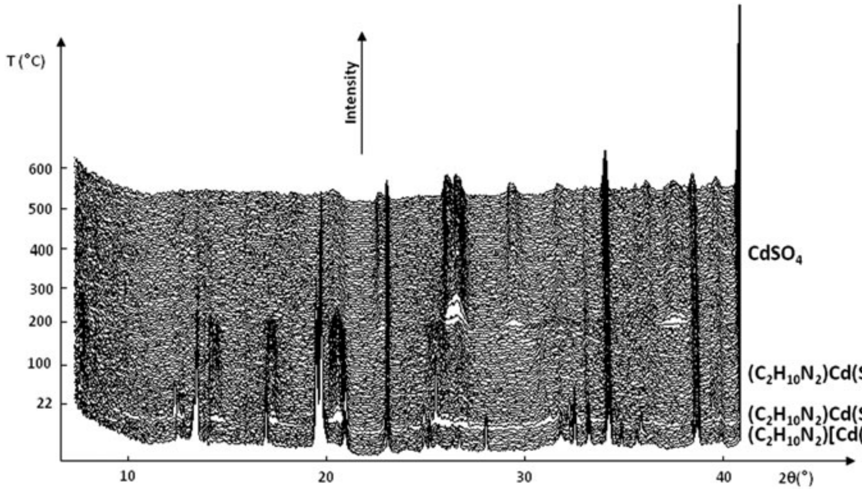

Figure 5. TDXD plot for the decomposition of **1** in air.

ethylenediammonium sulfate leading to formation of the cadmium sulfate (observed weight loss, 52.33%; theoretical weight loss, 52.42%). This result is confirmed by the appearance of the diffraction lines relative to $CdSO_4$ in the TDXD plot at 340 °C.

3.2.2. $(C_4H_{12}N_2)[Cd(H_2O)_6](SO_4)_2$ (2). The thermogravimetry curve obtained during the decomposition of $(C_4H_{12}N_2)[Cd(H_2O)_6](SO_4)_2$ (**2**), from 30 to 600 °C, under flowing air is shown in figure 6. Decomposition is complex and takes place in three stages giving cadmium sulfate. The dehydration of the supramolecule takes place. The first weight loss occurs between 62 and 80 °C and corresponds to loss of two water molecules (observed weight loss, 6.8%; calculated weight loss, 7.18%). The intermediate tetrahydrate compound is not stable and decomposes immediately by loss of three water molecules leading to a

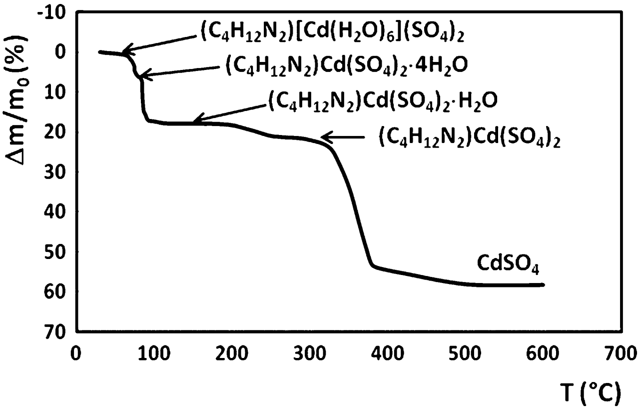

Figure 6. TG curve for the decomposition of **2** in air.

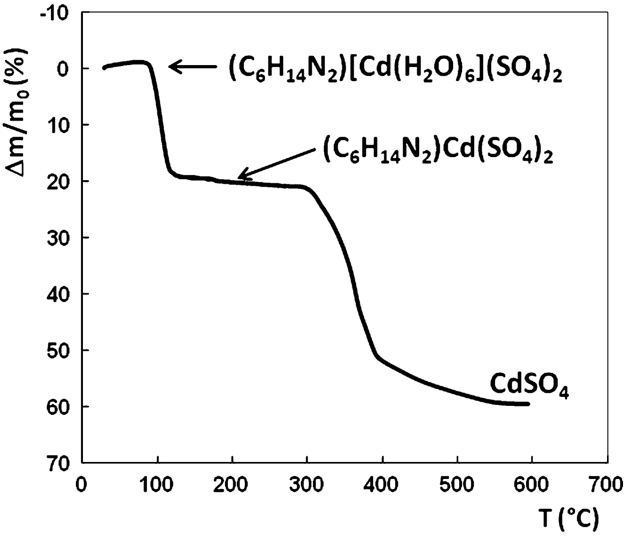

Figure 7. TG curve for the decomposition of **3** in air.

monohydrate phase (observed weight loss, 17.63%; calculated weight loss, 17.97%) stable to 190 °C. At this temperature, the last step of dehydration starts by loss of the remaining water molecule giving the anhydrous phase. The observed weight loss at 250 °C of 21.21% is in agreement with that calculated for full dehydration by the loss of six water molecules, 21.56%. The next and last stage of the decomposition corresponds to loss of the piperazinediium sulfate leading to the formation of cadmium sulfate (observed weight loss, 58.27%; theoretical weight loss, 58.31%).

3.2.3. $(C_6H_{14}N_2)[Cd(H_2O)_6](SO_4)_2$ (3). Figure 7 shows the thermogravimetry curve obtained during decomposition of **3**, from 30 to 600 °C, under air with a heating rate of 5 °C min^{-1}. Thermal decomposition of **3** is very simple and takes place in two steps. The first, starting at 68 °C, is attributed to full dehydration of the supramolecular complex (observed weight loss at 200 °C, 20.26%, calculated 20.50%). Decomposition of the anhydrous phase occurs from 280 to 530 °C by loss of the dabcodiium sulfate (observed weight loss, 59.47%; calculated weight loss, 60.36%).

4. Conclusion

Three hybrid materials containing cadmium, sulfate, and protonated diamine (ethylenediamine, piperazine, or dabco) have been synthesized and crystallographically characterized. Although they crystallize in two crystal systems, triclinic and monoclinic, three types of structures have been compared. The thermal decompositions depend on the amino group involved in the structure. Although the decompositions of the three compounds lead to cadmium sulfate, the compounds present different thermal behaviors, in the dehydration stage, which gives intermediate hydrates and anhydrous phases, which can be amorphous to X-rays in some cases, and crystalline in others. According to this work and our previous studies, dehydration of the supramolecular hybrid material containing ethylenediamine leads usually to a crystalline anhydrous phase stable in a wide range of temperatures.

Supplementary material

Details of the crystal structure investigations can be obtained free of charge from the Cambridge Crystallographic Data Center via www.ccdc.cam.ac.uk/data_request/cif. The deposition numbers are CCDC 979717 and CCDC 979722 for **2** and **3**, respectively.

Acknowledgement

Grateful thanks are expressed to Dr T. Roisnel (Centre de Diffractométrie X, Université de Rennes I) for the assistance in single-crystal X-ray diffraction data collection.

References

[1] L.F. Kirpichnikova, E.F. Andreev, N.R. Ivanov, L.A. Shuvalov, V.M. Varikash. *Kristallografiya*, **33**, 1437 (1988).
[2] A.N. Holden, B.T. Matthias, W.J. Merz, J.P. Remeika. *Phys. Rev.*, **98**, 546 (1955).
[3] N. Galešić, V.B. Jordanovska. *Acta Crystallogr. Sect. C*, **48**, 256 (1992).
[4] L.F. Kirpichnikova, L.A. Shuvalov, N.R. Ivanov, B.N. Prasolov, E.F. Andreyev. *Ferroelectrics*, **96**, 313 (1989).
[5] A. Pietraszko, K. Lukaszewicz, L.F. Kirpichnikova. *Polish J. Chem.*, **67**, 1877 (1993).
[6] M.-C. Daniel, D. Astruc. *Chem. Rev.*, **104**, 293 (2004).
[7] P. Dastidar, T.N. Guru Row, B.R. Prasad, C.K. Subramanian, S. Bhattacharya. *J. Chem. Soc., Perkin Trans.*, **2**, 2419 (1993).
[8] S. Bhattacharya, P. Dastidar, T.N. Guru Row. *Chem. Mater.*, **6**, 531 (1994).
[9] R. Kadirvelraj, A.M. Umarji, W.T. Robinson, S. Bhattacharya, T.N. Guru Row. *Chem. Mater.*, **8**, 2313 (1996).
[10] R. Kadirvelraj, S. Bhattacharya, T.N. Guru Row. *J. Inclusion Phenom. Mol. Recognit. Chem.*, **30**, 321 (1998).
[11] T. Bataille, D. Louër. *J. Mater. Chem.*, **12**, 3487 (2002).
[12] Y. Xing, Y. Liu, Z. Shi, H. Meng, W. Pang. *J. Solid State Chem.*, **174**, 381 (2003).
[13] T. Bataille, D. Louër. *J. Solid State Chem.*, **177**, 1235 (2004).
[14] C. Ruiz-Valero, C. Cascales, B. Gomez-Lor, E. Gutierrez-Puebla, M. Iglesias, M. Monge, N. Snejko. *J. Mater. Chem.*, **12**, 3073 (2002).
[15] A. Norquist, M.B. Doran, P.M. Thomas, D. O'Hare. *Dalton Trans.*, 1168 (2003).
[16] Y. Xing, Z. Shi, G. Li, W. Pang. *Dalton Trans.*, 940 (2003).
[17] C.N. Morimoto, E.C. Lingafelter. *Acta Crystallogr. Sect. C*, **26**, 335 (1970).
[18] M. Doran, A.J. Norquist, D. O'Hare. *Chem. Commun.*, 2946 (2002).
[19] M. Dan, J.N. Behera, C.N.R. Rao. *J. Mater. Chem.*, **14**, 1257 (2004).
[20] H. Naïli, W. Rekik, T. Bataille, T. Mhiri. *Polyhedron*, **25**, 3543 (2006).
[21] S. Yahyaoui, W. Rekik, H. Naïli, T. Mhiri, T. Bataille. *J. Solid State Chem.*, **180**, 3560 (2007).
[22] W. Rekik, H. Naïli, T. Mhiri, T. Bataille. *J. Chem. Crystallogr.*, **37**, 147 (2007).
[23] W. Rekik, H. Naïli, T. Mhiri, T. Bataille. *Mater. Res. Bull.*, **43**, 2709 (2008).
[24] W. Rekik, H. Naïli, T. Mhiri, T. Bataille. *Acta Crystallogr.*, **E65**, m1404 (2009).
[25] W. Rekik, H. Naïli, T. Mhiri, T. Bataille. *Solid State Sci.*, **11**, 614 (2009).
[26] Nonius. *Kappa CCD Program Software*, Nonius BV, Delft (1998).
[27] Z. Otwinowski, W. Minor. In *Methods in Enzymology*, C.W. Cater, R.M. Sweet (Eds), Vol. 276, p. 307–326, Academic Press, New York, NY (1997).
[28] P. Coppens. In *Crystallographic Computing*, F.R. Ahmed, S.R. Hall, C.P. Huber (Eds), p. 255–270, Munksgaard Publishers, Copenhagen (1970).
[29] L.J. Farrugia. *J. Appl. Crystallogr.*, **32**, 837 (1999).

[30] G.M. Sheldrick. *SHELXS-97, Programs for Crystal Solution*, University of Göttingen, Göttingen, Germany (1997).

[31] G.M. Sheldrick. *SHELXL-97, Programs for Crystal Structure Refinement*, University of Göttingen, Göttingen, Germany (1997).

[32] W. Rekik, H. Naïli, T. Mhiri, T. Bataille. *Acta Crystallogr.*, **E67**, m1176 (2011).

[33] S. Chaabouni, S. Kamoun, A. Daoud, T. Jouini. *Acta Crystallogr.*, **C52**, 505 (1996).

[34] P. Held. *Acta Crystallogr.*, **E59**, m197 (2003).

[35] I.D. Brown. *J. Appl. Crystallogr.*, **29**, 479 (1996).

[36] H. Naïli, W. Rekik, T. Bataille, T. Mhiri. *Polyhedron*, **25**, 3543 (2006).

[37] International Centre for Diffraction Data. *Powder Diffraction File*, Newtown Square, PA (2002).